Experimental investigation of the passage of fuel droplets through a spherical two-phase flame

Romain Thimothée, Christian Chauveau, Fabien Halter, Iskender Gökalp

▶ **To cite this version:**

Romain Thimothée, Christian Chauveau, Fabien Halter, Iskender Gökalp. Experimental investigation of the passage of fuel droplets through a spherical two-phase flame. Proceedings of the Combustion Institute, 2017, 36 (2), pp.2549 - 2557. 10.1016/j.proci.2016.08.031 . hal-01858463

HAL Id: hal-01858463
https://hal.science/hal-01858463v1

Submitted on 2 May 2024

HAL is a multi-disciplinary open access archive for the deposit and dissemination of scientific research documents, whether they are published or not. The documents may come from teaching and research institutions in France or abroad, or from public or private research centers.

L'archive ouverte pluridisciplinaire **HAL**, est destinée au dépôt et à la diffusion de documents scientifiques de niveau recherche, publiés ou non, émanant des établissements d'enseignement et de recherche français ou étrangers, des laboratoires publics ou privés.

Experimental investigation of the passage of fuel droplets through a spherical two-phase flame

R. Thimothée, C. Chauveau*, F. Halter, I. Gökalp

*Institut de Combustion, Aérothermique, Réactivité et Environnement (ICARE), CNRS-INSIS, 1C Avenue de la Recherche Scientifique, 45071 Orléans Cedex 2, France

Abstract

This paper reports experimental studies of two-phase combustion carried out with an aerosol of mono-sized ethanol droplets generated by rapid expansion under microgravity conditions. Optical diagnostics consisting of coupling laser tomography with the high-speed ILIDS technique are successfully applied for the aerosol combustion study. Droplet diameter reduction together with the radial droplet displacement ahead of the flame front is accurately measured. It is found that fuel droplets evaporate by following the d^2 law which confirms the validity of this model in an aerosol configuration. The laser tomography technique allows the identification of droplets which are present in the burnt gases. A regime diagram has been built using relevant non-dimensional parameters of two-phase combustion to exhibit the observations of droplets crossing. The results demonstrate that the droplet size and the droplet interdistance are the most important parameters which control the possibility for the droplet to penetrate the burnt gases. Moreover, it is observed that typical topologies of flames in terms of size and number of cells are related to the droplet number density.

Keywords: Aerosol combustion, droplet evaporation, droplet velocity, flame front interaction, flame instabilities

1. Introduction

Real energy conversion systems are characterized by poly dispersed sprays and turbulent flows but simplified configurations are required to identify the effects of all the parameters. Fundamental studies on flame propagation in a droplet cloud or aerosol are essential for a better understanding of many practical applications including spark ignition (SI) engines, gas turbines and industrial

*Corresponding author. Address: Institut de Combustion, Aérothermique, Réactivité et Environnement (ICARE), CNRS-INSIS, 1C Avenue de la Recherche Scientifique, 45071 Orléans Cedex 2, France. *E-mail address:* christian.chauveau@cnrs-orleans.fr (C. Chauveau).

furnaces. Burgoyne and Cohen [1] are among those who initiated such studies. They identified two separate regimes: for droplet diameters below 10 µm, combustion was similar as in a gas phase, while above 40 µm, each droplet burned individually. Later Mizutani and Nakajima [2] examined the effect of adding kerosene droplets in a propane-air premixture. They found that propane flames were markedly accelerated by the presence of kerosene droplets. Hayashi and Kumagai [3] developed a reliable technique to generate an aerosol of nearly monosized droplets in a stagnant premixture with the vapor and droplets being the same fuel. Later, Hayashi et al. [4] observed the same flame speed promotion for ethanol flames due to the presence of small droplets and they also showed that, for sufficiently large droplet diameters, two-phase flames develop cellular instabilities on their surface. Similar observations have been reported using the same technique of rapid expansion by Lawes et al. [5] and also during experiments performed under microgravity conditions [6, 7].

Atzler et al. [8] observed that the presence of droplets in an iso-octane aerosol causes instabilities in terms of flame speed oscillations. The cyclic variation of the flame speed has been explained with reference to the droplet inertia which induces differences between droplet velocities and the gas velocity near the flame front resulting in local equivalence ratio variations. The equivalence ratio of the gas phase may change considerably and sometimes conduct to the flame extinction. The works of Stapf et al. [9] on spray combustion modeling in a diesel engine, pointed out that group combustion effects have a dominant influence on spray combustion. They showed that large droplets create stratification in the gas phase where the local equivalence ratio can be inferior to the flammability limit while the droplets in groups evaporate quickly generating ignitable premixed fuel–air zones. More recently, Bradley et al. [10] demonstrated that for sufficiently large fuel droplets and rich mixtures, droplets may enter the reaction zone and further enhance existing gaseous flame instabilities by significantly increasing the entrained fuel mass flux. The presence of droplets considerably complicates combustion by introducing vaporization, aerodynamics and mixing processes, heterogeneous combustion with different combustion regimes together with flame instabilities.

This paper aims to enhance the comprehension of spray combustion by specifically focusing on the possibility for fuel droplets to cross the flame front. The objectives are therefore to identify the conditions for the presence of droplets in the burned gases and to investigate the parameters to be taken into account to correctly predict the potential crossing of fuel droplets through the flame front.

Mono-sized and homogeneous ethanol aerosols are generated using the rapid expansion technique [3, 5] in a dual chamber under reduced gravity conditions. High fidelity optical diagnostics are successfully applied to two-phase combustion and new experimental data were measured with a temporal resolution during the combustion process (evaporation rate, droplet displacement and

droplet diameter reduction). Experimental diagrams are built in order to highlight the relevant parameters of the observed passage of droplets and the possible influence on the two-phase flame instabilities is also discussed.

2. Experimental setup and procedures

2.1 Dual chamber

The experiments are conducted in a 1 L spherical combustion chamber which is centered in a high-pressure chamber of 11 L. The combustion chamber is equipped with 8 symmetrically distributed evacuation valves to release pressure during the flame propagation. The combustion chamber is filled with the flammable mixture while the high-pressure chamber is simultaneously filled with nitrogen at the same pressure, ensuring proper sealing. When the pressure inside the combustion chamber increases, the evacuation valves open and remaining flammable gases are evacuated toward the high-pressure chamber to be mixed with nitrogen and ensure a totally inert mixture. A schematic of the experimental facility is given in Fig. 1.

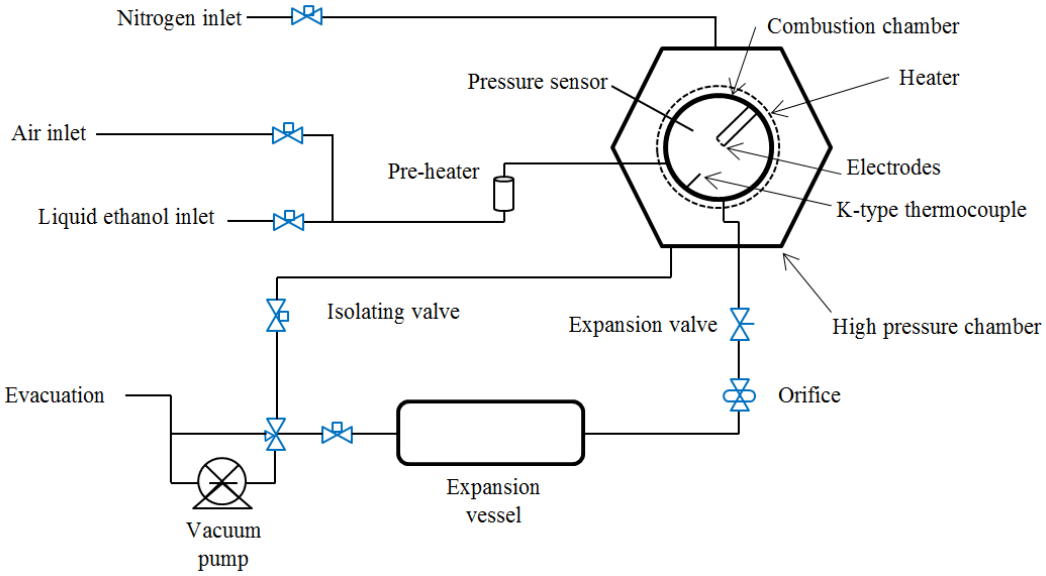

Fig. 1. Schematic representation of the experimental facility.

Liquid fuel injection is performed using a multi-injection system with a switching valve which delivers an accurate volume of ethanol to obtain the targeted equivalence ratio. The fresh gases are heated by an electric heating cable that encircles the chamber. Additionally, a preheater is used to pre-vaporize the air-fuel mixture before its arrival in the combustion chamber. In all cases, the initial mixture injected in the combustion chamber is fully vaporized.

2.2 Creation of the fuel aerosol

The fuel aerosol is generated from this gaseous air-fuel mixture. The chamber is connected to an expansion vessel of 2.5 L, initially vacuumed, via an expansion valve and an adjustable orifice (see Fig. 1). The opening of the expansion valve induces a fast pressure drop in the combustion chamber (ΔP), also decreasing the temperature of the gaseous mixture. When the partial pressure of the fuel becomes greater than its saturation pressure, the wet regime is reached, causing the start of condensation and so the formation of fuel droplets. Once the target pressure has been achieved in the combustion chamber, the expansion valve closes. The aerosol may then be centrally ignited using two tungsten electrodes.

To avoid any disturbing effects of droplet settling and aerosol stratification, the experiments were conducted under reduced gravity conditions. These conditions were obtained using the parabolic flights of the CNES Airbus A310 ZERO-G, during which a 10^{-2}g gravity level is achieved.

A K-type thermocouple of 13 µm diameter and a pressure sensor monitor the temperature and the pressure during the filling process and during the expansion for aerosol formation (an example can be consulted in Fig. S1). Note that the initial temperature was fixed at 343K for all conditions. During expansion, only part of ethanol is condensed to create droplets meaning that at the moment of ignition, ethanol is present both in gaseous state and as droplets. Therefore the global equivalence ratio of the mixture can be defined as the sum of a liquid equivalence ratio Φ_l and a gaseous equivalence ratio Φ_g such as: $\Phi = \Phi_l + \Phi_g$.

3. Optical diagnostics

3.1 The shadowgraphy system

The two chambers possess two pairs of aligned transparent windows to allow optical access inside the combustion chamber from both sides. Firstly, a classical shadowgraphy system is employed in order to track the flame front displacements and to visualize the morphology of the flame surface. An Energetiq LDLS is used as the light source and a high-speed camera (Phantom v1210) continuously records the flame propagation at 15000 fps.

The temporal evolution of the flame radius $R_f(t)$ is obtained directly from the shadowgraphy images where a post-processing program was used to fit the flame front. The temporal derivation of the flame radius yields the flame propagation speed V_S such as: $dR_f(t)/dt = V_S(t)$. The unstretched flame propagation speed, noted V_S^0, is extracted by extrapolation to zero stretch of V_S versus the flame stretch rate $\kappa = 2 \cdot V_S/R_f$ using the non-linear model [11, 12]. More details about this

methodology can be found in [7]. Unstretched flame propagation speed will be used in the following to evaluate a chemical time useful in the diagram construction.

3.2 Coupling of laser tomography and ILIDS

Secondly, the shadowgraphy system was replaced by two laser diagnostics jointly used: laser tomography for locating the position of the droplets and an interferometry technique for determining the droplet size. Both diagnostics, set up on each side of the combustion chamber, require the creation of a planar laser light sheet at the center of the combustion chamber. A laser (Coherent Verdi) emitting a laser beam at 532 nm is used with an optical system consisting of lenses and a mirror, to generate a thin laser sheet of less than 250 µm thick. A light absorber disposed at the bottom of the combustion chamber limits the reflections on the walls. Two high-speed cameras (Phantom v1210 and v1611) are arranged on each optical access for use at high speed during the two-phase combustion process.

a. Laser tomography

A first camera focusing on the laser light sheet and equipped with an interference filter at 532 nm, receives the light scattered by the fuel droplets located in the laser sheet plane. Example of instantaneous tomography images are given as a Supplementary Material (Fig. S2). An acquisition rate of 19000 fps and a spatial resolution of 768×768 pixels^2 corresponding to a 40.5 mm side enable a precise tracking of the temporal evolution of the position of fuel droplets during flame propagation.

The high repetition rate of the tomography allows evaluating the radial velocity of each drop behind the flame front through the application of a Particle Tracking Velocimetry processing.

b. High-speed ILIDS

A second camera is set on the other side of the combustion chamber to evaluate simultaneously the droplets size evolution by Interferometric Laser Imaging for Droplet Sizing (ILIDS). With this system, an interference fringe pattern is obtained from each droplet when the image plane is defocused. By using optical geometric properties [13, 14], it is possible to determine a relationship between the number of fringes N and the diameter of the droplet d. Due to the implementation constraints experiment, the camera axis is perpendicular to the laser plane. Reasonable resolution of

1.78µm/fringe is obtained with a Sigma lens of 180 mm focal length, positioned at 243 mm from the laser plane.

Measurements are performed on several droplets and the arithmetic average diameter D_{10} or the Mean Sauter Diameter was used.

The acquisition rate is set to 25000 fps with a spatial resolution of 768×768 pixels^2 on a square field of 28.5 mm side. The reduction of the number of fringes gives information on the decrease of the droplet size during the flame front propagation.

3.3 Aerosol characterization prior to ignition

As the droplet diameter, the number of droplets per unit volume is a prerequisite to correctly analyze the interaction between a flame and an aerosol. To complete the current analysis, the density number was characterized prior to ignition and during the aerosol formation in a previous study using a laser diffraction particle size analyzer (HELOS Sympatec) [15]. The number density was estimated by measuring the laser attenuation signal and by using the Beer-Lambert law. This system also provides droplets diameter information, which may be compared to those measured with the ILIDS technique.

Figure 2 shows a typical temporal evolution of the number density (blue solid line) during the expansion process for initially gaseous ethanol-air mixture (T_i=343K - P_i=0.4MPa - ΔP=0.15MPa - Φ=1.1). Acquisition is triggered by the opening of the expansion valve. The number of droplets per unit volume sharply increases and remains constant after few seconds. Temporal Sauter Mean Diameter evolutions recorded with laser diffraction (black filled squares) and ILIDS technique (black open circles) are also reported in this figure.

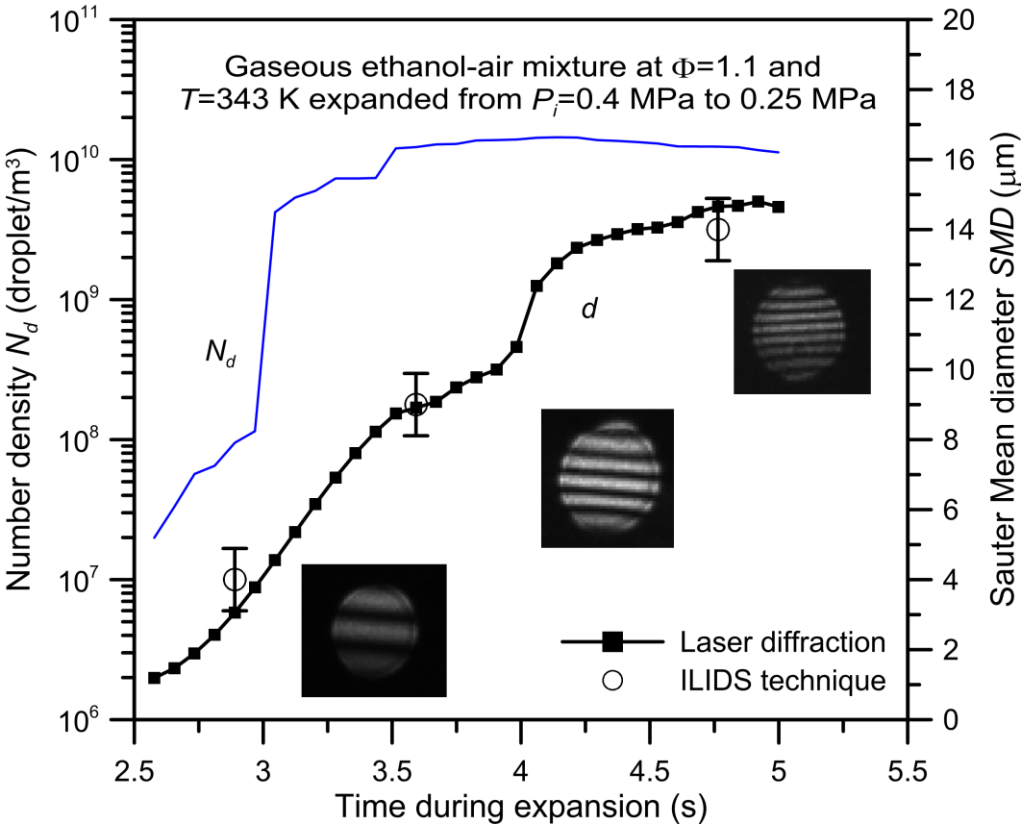

Fig. 2. Typical variations of the SMD and the number density with time during expansion.

Images of interference patterns are also shown in the figure to illustrate the drop size evolution. The drop size increases with the fringes number. Error bars correspond to the sensitivity of the fringes number on the diameter determination.

For this condition, the Sauter Mean Diameter (SMD) increases to reach 15 µm at the end of the expansion process. Very good agreement is observed between both techniques. High-speed ILIDS technique may be used during the flame propagation and its high temporal resolution enables to track droplets diameters during the combustion process. To avoid droplets vaporization, ignition should be triggered shortly after aerosol formation.

Droplet densities and mean diameters may be noticeably varied by changing the initial pressure P_i (between 0.35 MPa and 0.6 MPa), the pressure drop (ΔP between 0.12 MPa and 0.25 MPa) and the initial fuel quantity (global equivalence ratio from 0.7 to 1.45).

SMD increases with the initial fuel quantity and is not significantly influenced by the initial pressure although the number of droplets per unit volume increases with the initial pressure and remains almost constant with the fuel concentration. For more details, the reader is referred to [16].

In the current study, the SMD and the droplet density are varied respectively between 5 and 23 µm and between $1.5\cdot 10^{9}\ m^{-3}$ and $2.0\cdot 10^{11}\ m^{-3}$.

Now that initial conditions are controlled, the attention is focused on the droplet evolution during the flame propagation.

4. Results and analysis

4.1 Measurement of droplet size reduction ahead the flame front

In this section, the arithmetic average diameter D_{10} is used.

The Stokes number has been calculated for all conditions of aerosol experiments and was found to be far lower than unity. All droplets follow therefore the gas flow, which means that all droplets have low inertia and that evaporation is not impacted by any convection.

The temporal evolution of the average diameter is tracked using the high speed ILIDS technique and illustrated in Figure 3 (open circles). The experimental conditions (initial pressure and temperature, pressure drop and global equivalence ratio) are reported in the figure. Images of interference patterns are also shown in the figure. For this illustration, the fringes number decreases from 7 to 4 corresponding respectively to droplet diameters around 12 and 5 μm.

The diameter squared (filled circles) follows a linear trend, meaning that the droplets in the vicinity of the flame front follow the d^2 law model [17, 18]. This was the case for all conditions, even for dense aerosols.

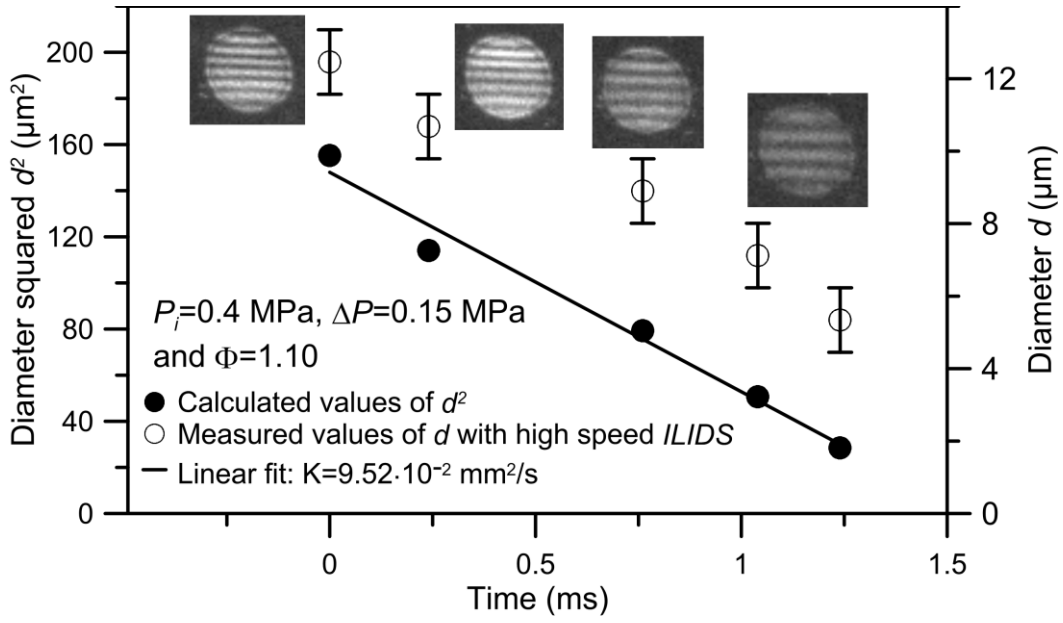

Fig 3. Illustration of the droplet size reduction ahead the flame front using high-speed ILIDS.

From droplet size reduction measurements, it is possible to determine the vaporization rate ($9.5 \cdot 10^{-2}\ mm^2/s$ for the conditions reported in Figure 3). Calculated values of evaporation rates will be

used later to estimate the droplets vaporization time. By taking into account the uncertainty on the droplet diameter and the error made by the interpolation calculation (least squared method), the maximum error on the evaporation rate is about 13%, which is acceptable for the present purpose.

4.2 Measurements of the droplet displacement and identification of the presence of fuel droplets in the burnt gases

When the flame propagates, fuel droplets initially motionless are set into motion by the expansion of the burnt gases. High frequency images obtained with laser tomography are used to measure the radial displacement of each drop in front of the flame front using a PTV treatment (Particle Tracking Velocimetry). An area corresponding to a crown with a typical width of 4-5 mm is considered for the PTV treatment. Unlike the fresh gases undergo the expansion of the flame, burnt gases are at rest if not affected by the effects of radiation [19]. As a result, a particle crossing the reaction zone may be identified because of its change in velocity.

The trajectory of an individual droplet is illustrated in Figure 4. The experiment condition corresponds to an initial pressure of 0.6MPa, an initial temperature of 343K, a pressure drop of 0.25MPa and a global equivalence ratio of 0.8.

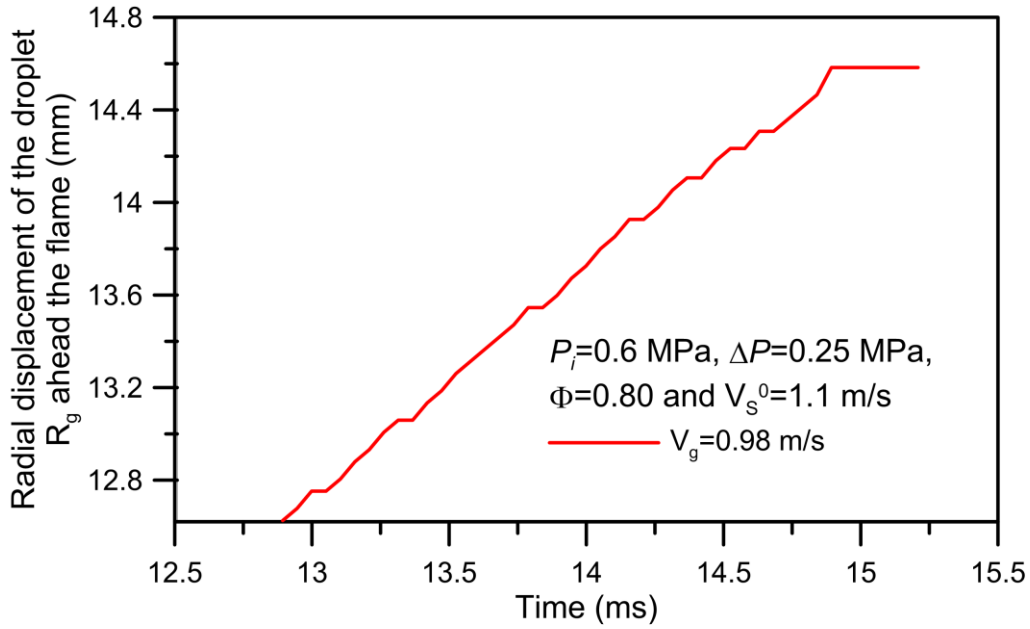

Fig. 4. Example of a measurement of a droplet displacement ahead the flame front.

For the sake of clarity, only the end of the droplet trajectory is reported on this figure. The droplet is moved over 2 mm by the flame expansion. Then, its position remains unchanged during less than 1 ms before full vaporization. The droplet is located in the burnt gases during the last part of the

vaporization process which is highlighted by the stagnation of the radial displacement ($dR_g(t)/dt = 0$).

For this individual droplet, an average velocity (V_g) is calculated from the almost linear part of the curve just before stagnation. In this case, the velocity of the droplet in the vicinity of the flame front is estimated at 0.98 m/s, which almost corresponds to the difference between the unstretched propagation speed (1.1 m/s) and the laminar flame speed (0.15 m/s), as indicated by Varea et al. [20]. Indeed, in our case, the unstretched propagation speed and laminar flame speed are respectively of 1.1 m/s and 0.15 m/s. The difference between these two speeds, which corresponds to the flame expansion, is relatively close to the droplet velocity.

Using this criterion of droplet immobility, three distinct behaviors of droplets ahead the flame may be identified. State 0: droplets evaporate progressively when they are pushed by the expanding gas and do not cross the flame; State 1: isolated droplets cross the flame and are found in the burnt gases without any movement; State 2: the droplets cross the flame grouped into packets (three to five) and are found in the burnt gas at rest.

In state 1, the aerosol behaves analogously to 0 but with droplets that detach from the aerosol in an isolated manner. State 2, reveals some packets of droplets that detach from the mist and form an indented aspect.

4.3 Regime diagrams from experimental observations

The purpose of this section is to value the experimental information described previously to identify the regimes where drops pass the flame front and continue their vaporization and eventually their oxidation in the burnt gases. This event may lead to an incomplete combustion and favored the formation of soot emissions. Chui et al. [21] were the first to propose a classification of two-phase flames in terms of burning regime. They demonstrated theoretically the importance of the competition between the droplet evaporation rate and the diffusion rate of the hot gases inside the cloud. These phenomena are directly related to the distance between the drops and their diameter. Later, Borghi [22] proposed a new level of analysis by introducing two characteristic times of two-phase combustion: the vaporization time τ_v and the chemical time of the flame τ_c. The ratio of these characteristic times can discriminate the droplets state in the vicinity of the flame front.

The Sauter Mean Diameter (SMD) values measured by laser diffraction are considered to be representative of the cloud. The droplets interdistance, denoted a, was evaluated using [23]: $a = 1/\sqrt[3]{N_d}$ (with N_d the density number). The characteristic chemical time is equal to: $\tau_c = \delta_L^0/S_L^0$. The

laminar flame thickness δ_L^0 is based on the maximal temperature gradient. S_L^0 is the laminar flame velocity.

Laminar flame thickness has been calculated with the PREMIX code of the CHEMKIN package and the kinetic scheme of Leplat et al. [24] in the aerosol thermodynamic conditions (pressure and temperature just prior ignition) and for the global equivalence ratio of the mixture, Φ. It is important to note that although the initial temperature was set at 343 K for all experimental conditions, the temperature just prior to ignition is lower and differ depending on the pressure release. Laminar burning velocity S_L^0 has been evaluated based on the experimental data of V_S^0 and the numerical determination of the expansion factor.

A vaporization time has been evaluated by considering the d^2 law in the aerosol as: $\tau_v = SMD^2/K$ with K the vaporization rate determined with ILIDS high-speed measurements (section 4.1) and by applying the correction factor related to the interaction effect between droplets depending on the ratio *a/SMD* [25].

The whole set of experiments performed for this study is reported in Fig. 5a. These experimental conditions correspond to initial pressures P_i between 0.35 MPa and 0.6 MPa, pressure drops between 0.15 MPa and 0.25 MPa and global equivalence ratios from 0.7 to 1.45. For each experimental condition, the four information describing the aerosol and the flame reactivity have been evaluated (a, SMD, δ_L^0 and S_L^0). Repeatability of the results was ensured by conducting 3 experiments for each condition.

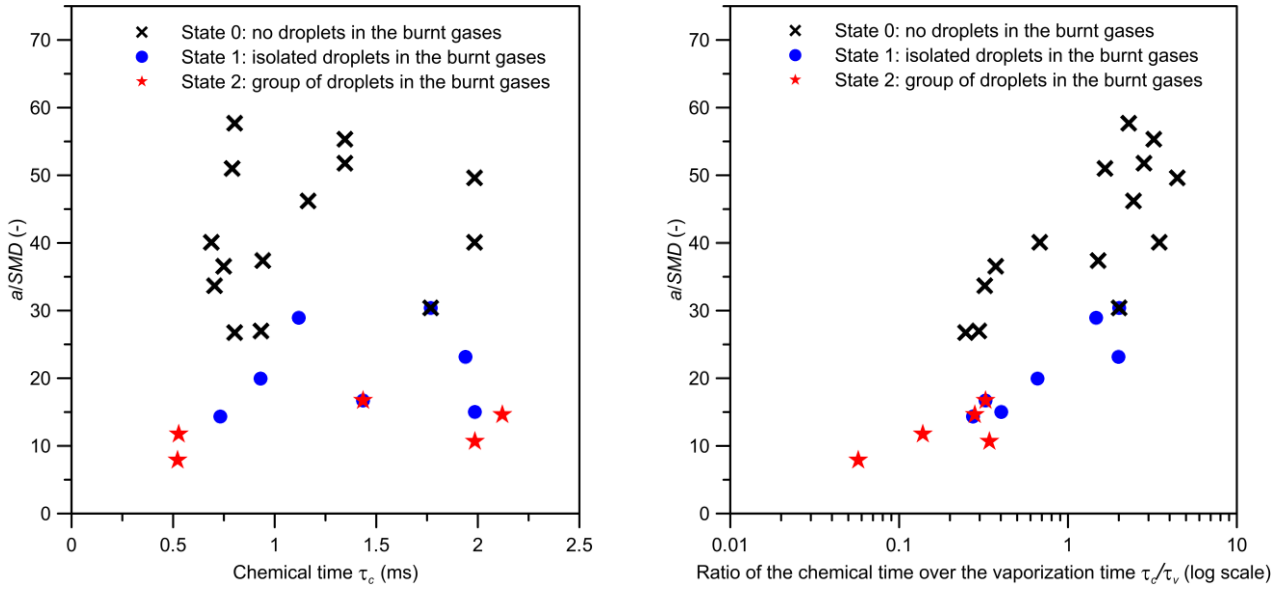

Fig. 5. Experimental diagram of the presence of fuel droplets in the burnt gases for different conditions of ethanol aerosol in function of a) the chemical time; b) the ratio of the chemical time to the vaporization time (log scale).

Additionally, each individual condition is classified between the three states previously identified. Figure 5a clearly shows the influence of droplet size and number density on the possibility of droplets passing the flame front. State 2 only appears for values of *a/SMD* below 20 and the upper limit for droplets to pass the flame front is around 30. It is interesting to note that the chemical time has little influence on the three transition states, even if the order of variation is relatively moderate. In order to add a new level of analysis, the ratio between the chemical and the vaporization times is considered.

This second diagram (Figure 5b) better highlights the three observed states. State 2 is observed for *a/SMD* less than 20 and for very large vaporization time versus the chemical time. Under these conditions, droplets are large and very close to each other. If τ_c/τ_v increases, droplets are more easily vaporized and rarely pass through the flame front. A ratio $of\ \ \tau_c/\tau_v > 2$ coupled with higher values of *a/SMD* lead to aerosol configurations with small droplets and far from each other. Under these conditions, droplets vaporize quickly and have no chance to pass through the reaction zone.

The theoretical limit separating a total and an incomplete evaporation corresponds to a ratio τ_c/τ_v equal to unity. However, experimental observations show that there are several cases identified as state 0 for values of $\tau_c/\tau_v < 1$ (and even close to 0.3) with *a/SMD* equal to 25.

All experimental observations of droplets crossings (states 1 and 2) have been mapped on the theoretical diagram of Borghi and Destriau [26], in order to compare the current results to an existing two-phase combustion diagram (this can be consulted on Supplementary Material, Fig. S3). It was found that the majority of cases identified as states 1 and 2 correspond to the regime of group combustion. Overall results are in good agreement with the theory of two-phase combustion, and the states of droplets passage are not related to the regimes of two-phase combustion. However, it seems that another parameter has to be considered in order to clarify this situation and that further investigations would be necessary.

4.4 Discussion of the two-phase flame topology

It is well established that a flame propagating through a fuel aerosol can develop cellular instabilities on its surface [5, 7]. It is of interest to investigate the relation between the possible presence of fuel droplets in the burnt gases and the topology of the two-phase flames. A major issue is that the prediction of the possibility of a two-phase flame to be unstable could be simply deduced from the knowledge of droplets crossing the flame. Different topologies have been observed in terms of flame shape, size and number of cells on the flame surface. It is found that flame morphology with big cells appear for diluted aerosols, whereas, flame surfaces with smaller structures appear for dense aerosols. Examples of flame morphology exhibiting these two kinds of topologies are shown in Fig.

6. Number density values are also reported, the SMD is about the same for the two cases. Current results show that flames are smooth and stable when the droplets are fully evaporated ahead the flame front while flames are cellular when droplets cross the reactive zone and are present in the burnt gases. However, these results suggest that the different types of cellularity in a two-phase flame are not necessarily related to the presence of fuel droplets isolated or in packets in the burnt gases.

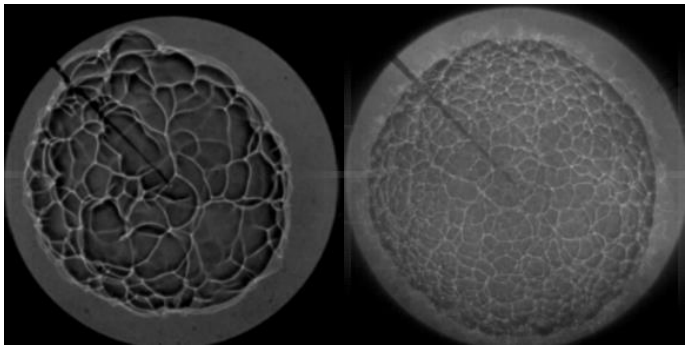

Fig 6. Shadowgraph images of two-phase flames exhibiting two different observations of morphology. Left: a flame surface with a few large cells at P_i=0.45 MPa, ΔP=0.12 MPa and Φ=1.35 with $N_d = 2.6 \cdot 10^{10}\ m^{-3}$; Right: a flame surface with a high number of small cells at P_i=0.55 MPa, ΔP=0.2 MPa and Φ=1.10 with $N_d = 2.0 \cdot 10^{11}\ m^{-3}$.

5. Conclusion

Optical diagnostics have been successfully employed in order to measure relevant parameters of two-phase combustion. Specifically, the coupling of laser tomography with high-speed ILIDS during two-phase combustion has been validated as a strong tool for the measurement of droplet size reduction ahead the flame front together with their displacement. New experimental data are provided and the main concluding remarks are the following:

- The measurements of the droplet diameter ahead the flame front reveals that the vaporization process in a cloud follows the d^2 law even for dense configurations.
- A vaporization rate has been extracted from the droplet diameter measurements.
- Measurements of the droplet displacement allow identifying, by a zero velocity, conditions for which it is possible for fuel droplets to enter the burnt gases zone. Three main droplet states were clearly highlighted: no droplet crossing; isolated droplets and groups of droplets in the burnt gases.
- Experimental results were then rearranged to identify the regimes where drops pass the flame front and continue their vaporization in the burnt gases. It was found that the droplet size together with the droplet interdistance play the major role. A criterion of *a/SMD*=30 was determined to ensure a full droplet evaporation.

- Further investigations are identified to be necessary to clearly highlight an eventual relation between the flame topology and the states of droplet crossings through the flame front. However, current results show that the droplet number density seems to determine the intensity of the cellular instabilities in terms of number and size of the cells.

Acknowledgments

This work was supported by a joint grant from the CNES and the Région Centre. The authors gratefully acknowledge the support of the CNES and the CNRS through the GDR MFA n°2799 for their financial support.

References

[1] J. Burgoyne, L. Cohen, P. Roy. Soc. Lond. A Mat. 225 (1162) (1954) 375-392.
[2] Y. Mizutani, A. Nakajima, Combust. Flame 20 (3) (1973) 351-357.
[3] S. Hayashi, S. Kumagai, Proc. Combust. Inst. 15 (1) (1975) 445-452.
[4] S. Hayashi, S. Kumagai, T. Sakai, Combust. Sci. Technol. 15 (5-6) (1977) 169-177.
[5] M. Lawes, Y. Lee, N. Marquez, Combust. Flame 144 (3) (2006) 513-525.
[6] H. Nomura, K. Izawa, Y. Ujiie, J.i. Sato, Y. Marutani, M. Kono, H. Kawasaki, Proc. Combust. Inst. 27 (2) (1998) 2667-2674.
[7] R. Thimothée, C. Chauveau, F. Halter, I. Gökalp, Characterization of Cellular Instabilities of a Flame Propagating in an Aerosol, Proceedings of the ASME Turbo Expo 2015, Montréal, Canada, 2015.
[8] F. Atzler, F. Demoulin, M. Lawes, Y. Lee, N. Marquez, Combust. Sci. Technol. 178 (12) (2006) 2177-2198.
[9] P. Stapf, H. Dwyer, R. Maly, Proc. Combust. Inst. 27 (2) (1998) 1857-1864.
[10] D. Bradley, M. Lawes, S. Liao, A. Saat, Combust. Flame 161 (6) (2014) 1620-1632.
[11] T. Tahtouh, F. Halter, C. Mounaïm-Rousselle, Combust. Flame 156 (9) (2009) 1735-1743.
[12] A. Kelley, C. Law, Combust. Flame 156 (9) (2009) 1844-1851.
[13] G. König, K. Anders, A. Frohn, J. Aerosol Sci. 17 (2) (1986) 157-167.
[14] C. Mounaïm-Rousselle, O. Pajot, Part. Part. Syst. Charact. 16 (4) (1999) 160-168.
[15] R. Thimothée, C. Chauveau, F. Halter, I. Gökalp, Experimental Investigation of the Mechanisms of Cellular Instabilities Developing on Spherical Two-phase Flames, 13th International Conference on Liquid Atomization and Spray Systems, Tainan, Taiwan, 2015.
[16] M. Nassouri, *Caractérisation expérimentale de la propagation d'une flamme laminaire dans un milieu diphasique à haute pression et en microgravité.*, PhD Thesis, Université d'Orléans, France, 2014.
[17] D.B. Spalding, Proc. Combust. Inst. 4 (1) (1953) 847-864.
[18] G. Godsave, Proc. Combust. Inst. 4 (1) (1953) 818-830.
[19] H. Yu, W. Han, J. Santner, X. Gou, C.H. Sohn, Y. Ju, Z. Chen, Combust. Flame 161 (11) (2014) 2815-2824.
[20] E. Varea, V. Modica, A. Vandel, B. Renou, Combust. Flame 159 (2) (2012) 577-590.
[21] H. Chiu, H. Kim, E. Croke, Proc. Combust. Inst. 19 (1) (1982) 971-980.
[22] R. Borghi, Lecture series-van Kareman Institute for fluid dynamics 2 (1996) I1-I39.
[23] A.R. Kerstein, C.K. Law, Proc. Combust. Inst. 19 (1) (1982) 961-969.
[24] N. Leplat, P. Dagaut, C. Togbé, J. Vandooren, Combust. Flame 158 (4) (2011) 705-725.
[25] C. Chauveau, F. Halter, I. Gökalp, Vaporization in three-dimensional droplet arrays : effects of the fuel vapor saturation, 10th International Conference on Liquid Atomization and Spray Systems, Kyoto, Japan, 2006.
[26] R. Borghi, M. Destriau, Combustion et les flammes, Editions Technip, Paris, France, 1998, p. 373.